

**DESIGN AND OPERATION OF A WIDE RANGE SEGMENTED GAMMA  
RAY SCANNING ASSAY INSTRUMENT FOR THE MEASUREMENT OF  
BOTH LOW AND INTERMEDIATE LEVEL WASTE**

John A. Mason, Marc R. Looman, Robert A. Price and Antony C. N. Towner  
ANTECH, A. N. Technology Ltd.  
Unit 6, Thames Park, Wallingford, Oxfordshire, OX10 9TA, England

Roger Kvarnström and Heidi Lampen  
Fortum Power and Heat Oy  
Loviisa Nuclear Power Plant  
PL23, Loviisa, Finland

**ABSTRACT**

This paper describes the design and operation of a Wide Range Segmented Gamma ray Scanning (WR-SGS) assay instrument for the measurement of both Low and Intermediate Level Waste (LLW and ILW) in 200 and 340 litre drums and other waste containers. The instrument employs a single shielded and collimated high purity germanium (HPGe) detector to quantify the radionuclide content of the waste. A novel feature of the instrument is the use of an automated variable aperture collimator, which allows the vertical segment height to be adjusted. Conventional SGS measurements may be performed where the drum is rotated and measured in vertical segments. Alternatively, faster measurement can be made using continuous helical scanning of the drum as it rotates. Very high activity drums can be measured through the use of the variable aperture collimator. A gamma ray emitting transmission source is used to correct for waste density. In place of a conventional shutter the shielded transmission source is moved to a shielded storage position to eliminate background radiation arising from the transmission source. Using this approach, higher activity transmission sources may be used in order to achieve adequate density corrections for higher density drums. The various features of the WR-SGS make it applicable to the measurement of both very low and very high activity waste drums as well as waste drums with a wide range of density. Results will be presented from a variety of test drum and waste drum measurements.

**INTRODUCTION**

As nuclear waste disposal regulations become more comprehensive worldwide, there is increasing pressure to make more accurate measurements of nuclear waste, especially at lower activity levels. Typically, waste ranges from very low activity in low-density matrices to high activity with a wide range of waste matrix density. There is a need for an SGS waste assay and sentencing instrument [1,2] to cover this extended range of applicability. The ANTECH Wide Range Segmented Gamma Scanner (WR-SGS, Model G3250-200) was developed to satisfy this requirement.

A photograph of the ANTECH WR-SGS can be seen in Figure 1. The instrument is installed and in operation in the waste measuring area of Loviisa Nuclear Power Plant in Finland. In order to meet the demanding measurement requirements the WR-SGS

incorporates several novel features. These include a variable aperture collimator (VAC), adjustable horizontal detector (FRONT and BACK) positions, a transmission source storage safe, and helical drum scanning. Other features include semi-automatic conveyor loading, an incorporated load cell for drum weight determination, and a solid state dose rate probe independent of the HPGe (High Purity Germanium) detector.

The system has been calibrated using point sources in matrices of differing density. As an SGS is designed to measure distributed sources, the calibration process has been modelled using the MCNP Monte Carlo simulation code [3]. In particular, the source distribution, collimation and detector crystal configuration have been included in the detailed MCNP modelling.

This paper describes features of the WR-SGS. Data is presented to demonstrate the performance of the instrument over a range of activity and matrix densities.



**Figure 1.** WR-SGS installed in the waste measurement room at Loviisa Nuclear Power Plant

## **NOVEL FEATURES OF THE WR-SGS**

### *Variable Aperture Collimator*

Two features are critical to extending the range of applicability of the WR-SGS. The first of these is the variable aperture collimator. Figure 2 is a diagrammatic representation of the MCNP model showing the three-matrix calibration drum and the collimator and detector assembly. The variable aperture collimator can be seen in front of the detector crystal and lead shield. The VAC consists of front and rear

tungsten plates, which move under motor control to change the size of the aperture opening. A diagram from the 3-D mechanical model can be seen in Figure 3.

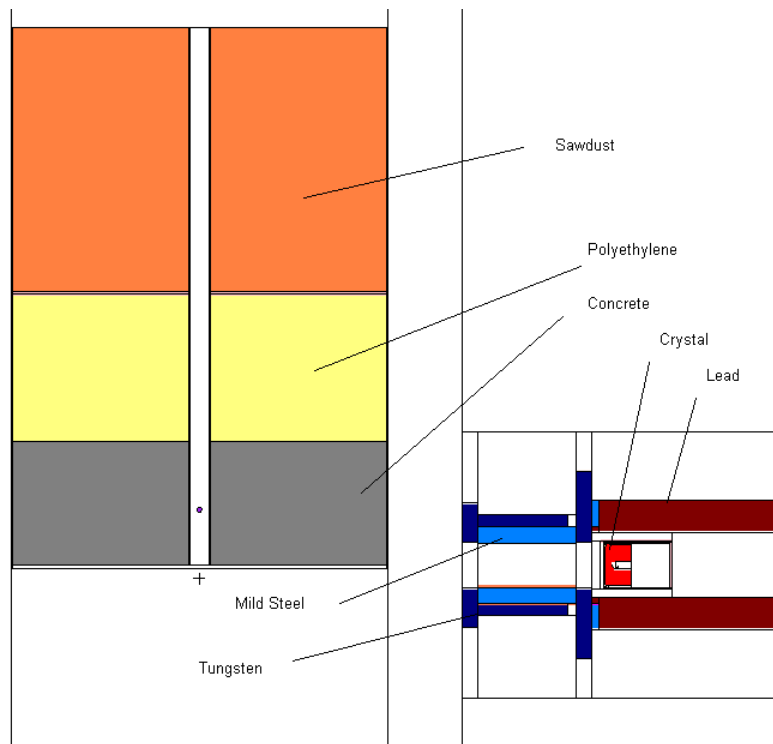


**Figure 2.** Vertical section of the MCNP model. On the left there is the 3-matrix calibration-test drum. On the right the collimator and detector assembly is shown. The Variable Aperture Collimator (VAC) opening is set to 70 mm. The VAC is positioned in the lowest scan position. The detector is shown in the FRONT position (closest to the drum).



**Figure 3.** Variable Aperture Collimator (VAC)

Typically, three VAC openings are employed in routine operation: 70 mm, 14 mm and 3.5 mm. A separate calibration is required for each VAC aperture setting. However, it is possible to use different VAC aperture settings for transmission and emission measurements. In this way, a low-density drum can be measured with a strong transmission source using the 3.5 mm aperture and the emission measurement,

where the drum activity is low, can be made with the 70 mm aperture. Alternatively, for very active drums, both transmission and emission measurements can be made with a smaller aperture. In this way, the range of applicable drum density and drum activity is extended. In operation, drum density is estimated using the weight measurement and overall drum activity is determined using the dose rate probe during a pre-scan measurement of the drum. This pre-scan information is then used to choose appropriate VAC apertures for both the transmission and emission measurements. Although the WR-SGS is normally operated in two-pass mode (separate transmission and emission measurements) it can also operate in one-pass mode (with a single combined transmission and emission measurement, where appropriate).

#### *Transmission Source Safe*

The second novel feature is the transmission source safe. In order to make low activity measurements with the lowest possible background it is necessary to eliminate background radiation arising from the transmission source. This is because even with the use of a shutter mechanism, a strong transmission source will make a significant contribution to the radiation background. When the source in the WR-SGS is not in use it is removed to a lead and tungsten shielded storage position. The WR-SGS at Loviisa employs Eu-152 transmission sources with a total activity of 30 mCi (1.11 GBq). When the source is located in the shielded store or safe the HPGe detector is not able to see any gamma-rays from the higher energy peaks of the transmission source. This means that at the low activity end of the measurement range the unit is able to sentence waste to the exempt category. This feature, when used in combination with the VAC, allows a strong transmission source to be employed to measure the transmission through low and very high-density matrices. Figure 4 shows the tungsten shielded transmission source holder descending into the shielded storage safe. Note that in the event of a power failure or emergency stop the source returns to the source safe under gravity in a controlled manner.



**Figure 4.** Tungsten shielded transmission source descending into the transmission source safe.

#### *Helical Scanning*

The WR-SGS can operate in conventional fixed-segment mode or in helical scanning mode for both emission and transmission measurements. In helical scanning mode the segment size is determined by a combination of the VAC aperture, the speed of scanning, and the data acquisition or data grab time for each spectrum measurement.

As with conventional SGS operation, each segment must correspond to a number of complete drum revolutions; typically this is two or four revolutions per helical scanned segment. The helical scanning process produces results, which are entirely equivalent to those obtained from fixed scanning. It does, however, have the advantage of a reduced measurement time as data is acquired while the detector is in motion. For successful helical scanning attention must be paid to ensure that micro-phonetic noise in the detector is minimised.

#### *Forward and rear detector positions*

Another simple feature that extends the measurement range to higher dose rate drums involves the physical movement of the detector and scanning assembly from a forward (FRONT) to a rear (BACK) position. This facility is employed when the dose rates are sufficiently high to result in high HPGe detector dead time even with the small 3.5 mm collimator aperture.

### **VALIDATION OF THE MONTE CARLO SIMULATION**

The WR-SGS has been calibrated and its performance assessed using point sources. In reality, Segmented Gamma Scanners are designed to measure distributed sources. In order to validate the use of point sources for calibration and testing, the point source measurements have been simulated using the MCNP code. This process involves simulating not only the geometry and position of the point sources but also the collimator shield and the detector crystal. Figure 5 is a plot of the measured and simulated detection efficiency of the system using a calibrated Eu-152 source in an empty drum (void matrix). The experimental efficiency data is obtained by dividing the measured net peak area of the main Eu-152 gamma ray peaks by the number of photons emitted per second for each peak. The experimental and simulated data is in very good agreement, as can be seen in Figure 5.

A calibration test drum with three regions of different density was constructed to facilitate testing in different matrices. The three matrices represented in the drum are sawdust (nominal density 0.15), polyethylene (nominal density 0.811) and concrete (nominal density 2.323). Detection efficiency measurements have been made in each of these three matrices and compared with simulated data in Figures 6, 7 and 8. It can be seen that the measured and simulated data is in very good agreement for these measurements.

In order to confirm that the simulated data is correct a comparison between measured and simulated data for point source detection efficiency measurements is presented in Table 1. This has been done for the three different matrices employed for measurement validation. Point source measurements in sawdust, polyethylene and concrete matrices are included in the table with the source positioned in three radial locations: 0 radius, 2/3 radius and on the periphery of the drum at 1 radius. Table 1 includes the ratio of the simulated to measured efficiencies. The measured and simulated data is in good agreement, with the exception of the peripheral position measurements in polyethylene. These slightly poorer results can be attributed to the fact that the polyethylene matrix density was not uniform with a lower density in the outer regions. This effect was not captured in the MCNP modelling.

R=0, Z=432 mm, VOID Drum

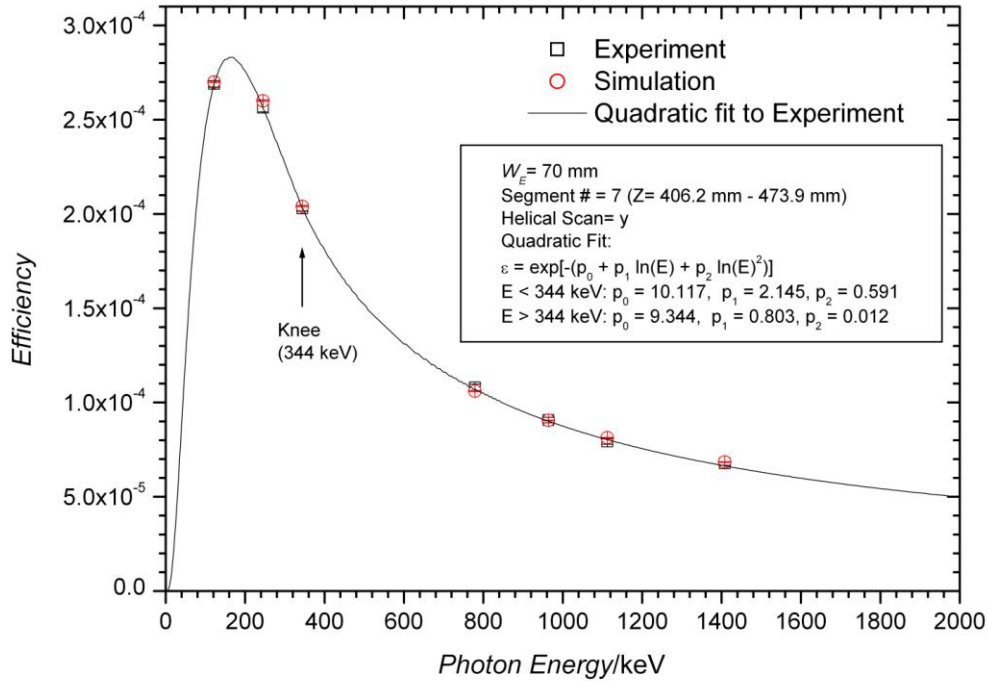


**Figure 5.** Experimental and simulated detection efficiency as a function of photon energy. The experimental data points are obtained by dividing the measured net peak area of the main Eu-152 peaks by the number of photons emitted per second for each peak. The Eu-152 source was placed centrally and at the mid height of a void drum. Helical scanning was selected for this particular scan, and the results are given for the seventh layer (the detector moved from 406.2 to 473.9 mm while the drum was rotated twice). The collimator opening was set to 70 mm and the detector pillar was positioned in the Front position. Due to the central radial position, it was not necessary to include drum rotation in the simulation. It was sufficient to calculate the efficiency at various heights to obtain the final result by averaging. The results of a quadratic fit are also given.

662 keV, R=0, Z=645 mm, 3-Matrix Drum

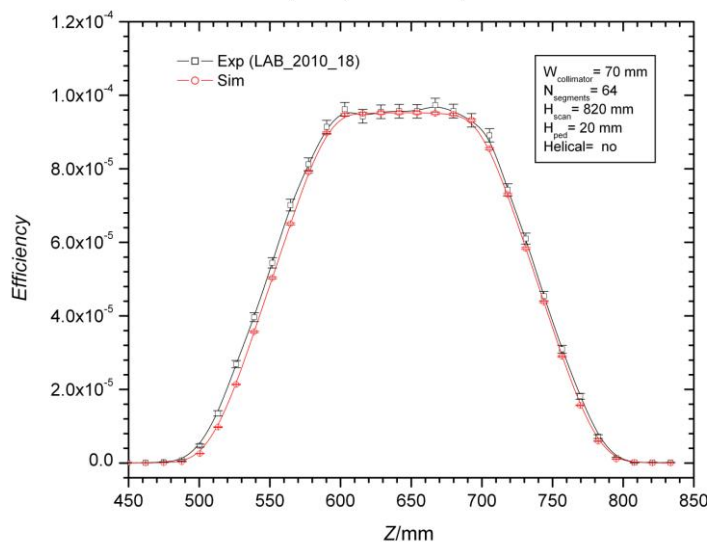


**Figure 6.** Detection efficiency for 64-segment discrete scan with the Cs-137 source (SI464) placed at the centre of the sawdust matrix.

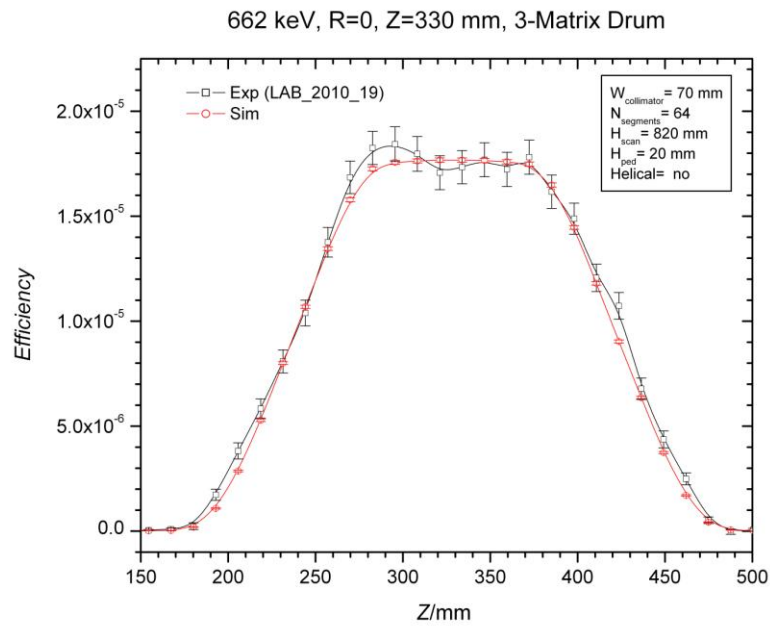


**Figure 7.** Detection efficiency for 64-segment discrete scan with the Cs-137 source (SI464) placed at the centre of the Polyethylene matrix.

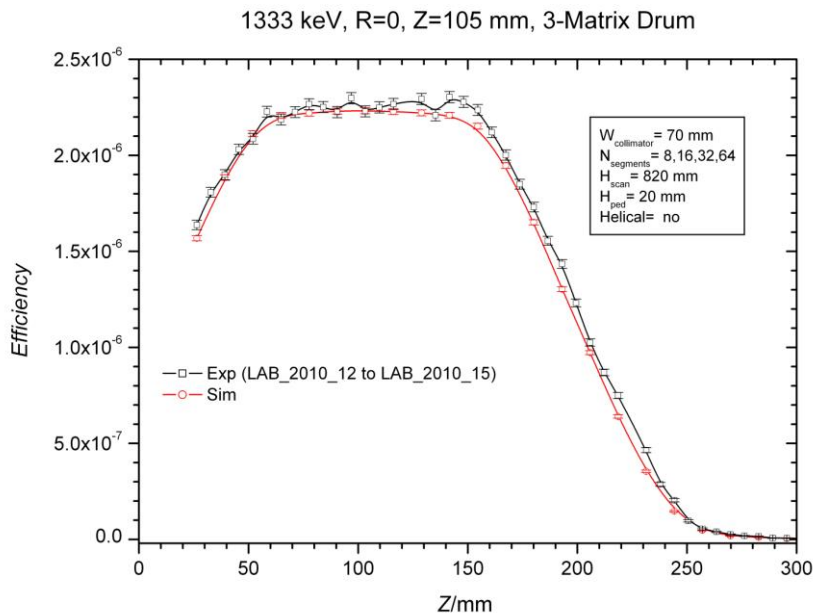


**Figure 8.** Detection efficiency for 64-segment discrete scan with the Co-60 source (SI461) placed at the centre of the concrete matrix.

ID	Matrix	Number of Segments $N_s$	Source			Simulated Efficiency $\epsilon_{Sim}$		Measured Efficiency $\epsilon_{Exp}$		$\epsilon_{Sim}/\epsilon_{Exp}$	
			Nuclide	Reference Activity $A_{ref}$ (Bq)	Pos.	Value	Error	Value	Error	Value	Error
40	Sawdust	13	Co-60	3.64E+04	0	1.45E-05	1.68E-08	1.54E-05	1.56E-06	0.94	0.10
44	Sawdust	13	Cs-137	6.96E+05	0	2.23E-05	2.09E-08	2.22E-05	7.30E-07	1.00	0.03
98	Sawdust	8	Co-60	3.64E+04	$^{2/3}R$	1.44E-05	6.93E-09	1.35E-05	1.43E-06	1.07	0.11
112	Sawdust	8	Cs-137	6.96E+05	$^{2/3}R$	2.23E-05	8.46E-09	2.27E-05	4.51E-07	0.98	0.02
99	Sawdust	8	Co-60	3.64E+04	R	1.42E-05	6.86E-09	1.36E-05	1.58E-06	1.04	0.12
51	Sawdust	13	Cs-137	6.96E+05	R	2.19E-05	8.42E-09	2.24E-05	4.54E-07	0.98	0.02
63	PE	13	Co-60	3.17E+07	0	4.31E-06	1.21E-08	4.36E-06	4.28E-08	0.99	0.01
46	PE	13	Cs-137	6.96E+05	0	4.09E-06	1.18E-08	3.97E-06	1.93E-07	1.03	0.05
62	PE	13	Co-60	3.64E+04	$^{2/3}R$	6.25E-06	5.93E-09	6.57E-06	1.10E-06	0.95	0.17
103	PE	8	Co-60	3.64E+04	R	8.04E-06	6.65E-09	9.57E-06	1.25E-06	0.84	0.13
116	PE	8	Cs-137	6.96E+05	R	1.11E-05	7.75E-09	1.25E-05	3.35E-07	0.89	0.03
67	Concrete	13	Co-60	3.17E+07	0	4.86E-07	4.06E-09	5.31E-07	1.07E-08	0.91	0.02
118	Concrete	8	Cs-137	6.96E+05	$^{2/3}R$	2.07E-06	3.41E-09	2.15E-06	8.83E-08	0.96	0.04
119	Concrete	8	Cs-137	6.96E+05	R	6.78E-06	6.08E-09	7.15E-06	2.53E-07	0.95	0.04

**Table 1.** For each SGS scan executed at the Loviisa Power Plant, with unique experiment ID, the measured and simulated average detection efficiencies are given. The set-up parameters of the scans are: the emission scan collimator opening (70 mm), the number of segments,  $N_s$ , the scan height (820 mm), the pedestal height (20 mm), the detector position (Front) and the number of rotations per segment (2). The source with source Reference Activity,  $A_{ref}$ , is placed at mid-height of the layer of interest of the 3-Matrix drum and at the indicated radial position (0,  $^{2/3}R$  and R). The tabulated errors are all for 2 sigma uncertainty. The ratio between the simulated and experimental efficiencies is also given.

## MEASUREMENTS OF SIMULATED MATRICES

The 220-litre calibration test drum has been employed to make a number of measurements with both cobalt and caesium sources of different strengths and in different radial positions around the drum. With these measurements, where point sources are used to simulate distributed sources, the measured activity is corrected based on correction factors determined by an MCNP analysis.

The results of a series of WR-SGS measurements conducted at Loviisa NPP in 2010 are given for a variety of Matrices (Sawdust, Polyethylene and Concrete) and the results are presented in Table 2. The tabulated data includes detector pillar position  $P$  (either F for Front or B for Back), and collimator opening settings  $w_E$  for Emission scan and  $w_T$  for transmission scan. The point sources with known reference activity,  $A_{ref}$ , were positioned in one of the three source tubes located at the following radial positions: centre (0), two-thirds of radius ( $^{2/3}R$ ) or full radius (R). During the pre-scan the Average and Peak Dose Rates are measured (only the peak dose rate is reported in the table). The transmission,  $T$ , for the actual matrix is given in percent. Note that in the analysis a volume source is assumed, however, the measurements are executed with a point source. The factor  $C_{PV}$  is used to calculate the apparent activity of a volume source with the same activity of a point source placed at a given radial position. After applying the correction factor the Corrected Activity,  $A_{cor}$ , is obtained. Finally, this Corrected Activity is compared to the Reference Activity and the relative measurement error is also given.



ID	Matrix	P	Collimator width (mm)		Source			Peak Dose Rate (micro-Sv/h)	T %	Measured Activity (Bq)		$C_{PV}$	Corrected Activity $A_{cor}$ (Bq)	$A_{cor}/A_{ref}$	
			$w_E$	$w_T$	Nuclide	Reference Activity $A_{ref}$ (Bq)	Pos.			Value	Error			Value	Error
40	Sawdust	F	70	3.5	Co-60	3.64E+04	0	0.3	65	3.73E+04	1.31E+03	0.95	3.53E+04	0.97	0.04
98	Sawdust	F	70	14	Co-60	3.64E+04	<sup>2</sup> / <sub>3</sub> R	0.2	68	3.34E+04	1.21E+03	0.95	3.17E+04	0.87	0.04
99	Sawdust	F	70	14	Co-60	3.64E+04	R	0.0	66	3.48E+04	1.23E+03	0.97	3.37E+04	0.93	0.04
44	Sawdust	F	70	3.5	Cs-137	6.96E+05	0	0.2	64	6.80E+05	6.79E+03	0.98	6.64E+05	0.95	0.01
112	Sawdust	F	70	14	Cs-137	6.96E+05	<sup>2</sup> / <sub>3</sub> R	0.1	67	6.49E+05	6.46E+03	0.98	6.33E+05	0.91	0.01
51	Sawdust	F	70	14	Cs-137	6.96E+05	R	0.2	66	6.75E+05	6.72E+03	0.99	6.69E+05	0.96	0.01
75	Sawdust	B	14	14	Co-60	3.17E+07	0	55.3	59	3.24E+07	1.52E+05	0.90	2.92E+07	0.92	0.00
63	PE	F	70	14	Co-60	3.17E+07	0	29.4	7.9	2.11E+07	6.98E+04	1.38	2.91E+07	0.92	0.00
62	PE	F	70	14	Co-60	3.64E+04	<sup>2</sup> / <sub>3</sub> R	0.3	12	3.46E+04	1.85E+03	0.95	3.29E+04	0.90	0.05
103	PE	F	70	14	Co-60	3.64E+04	R	0.2	7.3	4.47E+04	2.07E+03	0.74	3.31E+04	0.91	0.05
81	PE	B	14	14	Cs-137	6.96E+05	<sup>2</sup> / <sub>3</sub> R	0.2	6.3	7.01E+05	4.15E+04	1.06	7.43E+05	1.07	0.06
77	PE	B	3.5	3.5	Co-60	3.17E+07	<sup>2</sup> / <sub>3</sub> R	165.0	8.6	3.63E+07	2.89E+05	0.91	3.30E+07	1.04	0.01
67	Concrete	F	70	70	Co-60	3.17E+07	0	5.7	0.11	6.05E+06	4.77E+04	5.44	3.29E+07	1.04	0.01
118	Concrete	F	70	14	Cs-137	6.96E+05	<sup>2</sup> / <sub>3</sub> R	0.2	0.57	5.22E+05	1.77E+04	1.55	8.08E+05	1.16	0.03
119	Concrete	F	70	14	Cs-137	6.96E+05	R	0.4	0.54	1.72E+06	3.24E+04	0.47	8.12E+05	1.17	0.02
104	Concrete	F	14	14	Co-60	3.17E+07	0	6.7	0.56	6.48E+06	1.33E+05	4.70	3.05E+07	0.96	0.02
105	Concrete	F	14	14	Co-60	3.17E+07	<sup>2</sup> / <sub>3</sub> R	76.6	0.62	2.21E+07	2.46E+05	1.06	2.34E+07	0.74	0.01
69	Concrete	F	14	14	Co-60	3.17E+07	R	256.9	0.10	5.00E+07	2.12E+05	0.47	2.35E+07	0.74	0.00
79	Concrete	B	14	14	Cs-137	6.96E+05	0	0.4	0.14	3.07E+04	1.01E+04	16.1	4.94E+05	0.71	0.33
80	Concrete	B	14	14	Cs-137	6.96E+05	<sup>2</sup> / <sub>3</sub> R	0.2	0.11	5.47E+05	6.46E+04	1.66	9.08E+05	1.30	0.12
47	Concrete	F	70	70	Cs-137	6.96E+05	0	0.3	0.10	4.18E+04	4.06E+03	16.9	7.06E+05	1.01	0.10
59	Concrete	F	70	70	Cs-137	6.96E+05	<sup>2</sup> / <sub>3</sub> R	0.3	0.09	4.39E+05	1.35E+04	1.55	6.79E+05	0.98	0.03
106	Concrete	F	3.5	3.5	Co-60	3.17E+07	R	0.5	0.10	6.25E+07	9.16E+05	0.34	2.13E+07	0.67	0.01
78	Concrete	B	3.5	3.5	Co-60	3.17E+07	0	8.5	0.10	5.67E+06	1.96E+05	5.40	3.06E+07	0.97	0.03

**Table 2.** The results of a series of WR-SGS measurements conducted at Loviisa NPP in 2010 are given for a variety of matrices.

### MINIMUM DETECTIBLE ACTIVITY (MDA)

In order to determine the minimum detectable activity for a variety of different matrix densities, measurements were made with no sources present. In this way the MDA can be determined based on statistical criteria in relation to the background activity level. Measurements were made with matrix drums covering a wide range of densities from 0.1 up to 2.3 and with 1, 3 and 8 segments used in the analysis. The appropriate minimum MDAs were calculated for both Co-60 and Cs-137. The MDA criteria employed used the Currie Limit formulation based on two-sigma uncertainty [4].

The results of these measurements can be seen in Figure 9. The *3 segments*<sup>2</sup> data illustrated in Figure 9 is based on an extrapolation. It compares favourably with the measured *3 segments*<sup>1</sup> data, except at the lowest density. The *8 segments*<sup>1</sup> data has a higher MDA as the counting statistics for each segment are poorer and the MDA values are summed. For the low background environment at Loviisa NPP the WR-SGS is able to make routine measurements at a variety of matrix densities with a very low MDA.

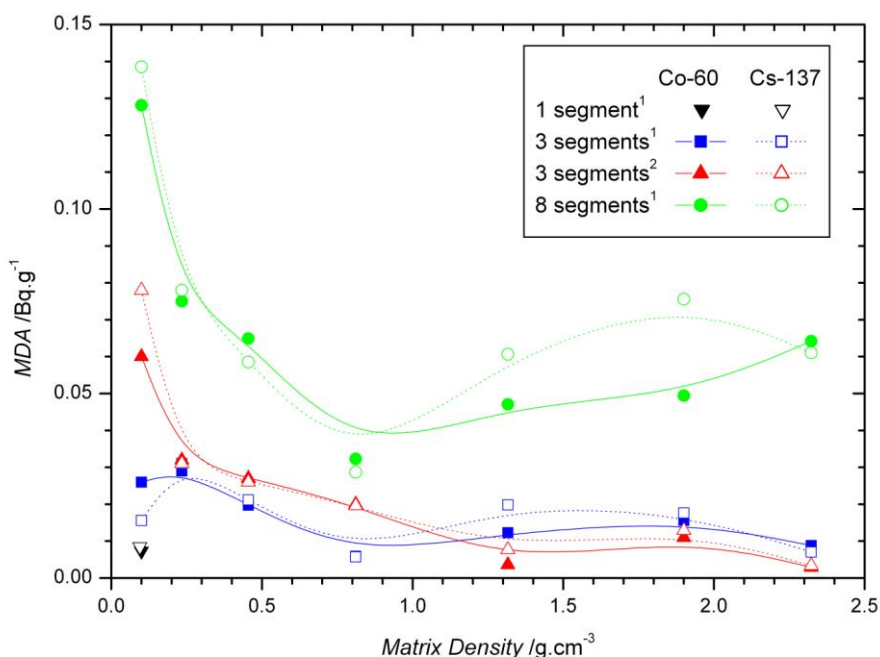


**Figure 9.** Plot of measured and calculated Minimum Detectable Activity (MDA) for a variety of matrix densities based on background measurements conducted at Loviisa NPP and using the Currie Limit convention with uncertainty of 2-sigma (95% confidence interval).

## CONCLUSIONS

This paper has described the new Wide Range Segmented Gamma Scanner (WR-SGS), which contains a number of novel features. Data from a range of measurements in different matrices is presented. It is evident that the WR-SGS extends the range of measurements that can be made with a conventional SGS to both lower and higher activity. With a high activity transmission source drums of high density greater than  $2 \text{ g/cm}^3$  may be measured. When operated in a low background environment appropriate low activity waste may be consigned to the exempt category.

The authors wish to thank Dr E. Ray Martin for helpful discussions.

## REFERENCES

- [1] E. R. Martin, D. F. Jones, and J. L. Parker, *Gamma Ray Measurements with the Segmented Gamma Scan*, Los Alamos Scientific Laboratory, LA-7059-M, 1977.
- [2] J. A. Mason, et. al., *A Tomographic Segmented Gamma Scanner for the Measurement of Decommissioning Wastes*, Proceedings of ICEM03, Examination School, Oxford, England, September 2003.
- [3] J. F. Briesmeister, *MCNP - A General Monte Carlo N-Particle Transport Code (Version 4C)*, Los Alamos National Laboratory, LA-13709-M, 2000.
- [4] L. A. Currie, *Limits for Qualitative Detection and Quantitative Determination*, Analytical Chemistry, 40 (3), p. 586-593, March 1968.